Journal of Hazardous Materials 161 (2009) 474–478

Contents lists available at ScienceDirect

Journal of Hazardous Materials

journal homepage: www.elsevier.com/locate/jhazmat

Application of Bayer red mud for iron recovery and building material production from alumosilicate residues

Wanchao Liu, Jiakuan Yang*, Bo Xiao

School of Environmental Science and Engineering, Huazhong University of Science and Technology (HUST), 1037 Luoyu Road, Wuhan, Hubei, 430074, PR China

ARTICLE INFO

Article history:
Received 5 December 2007
Received in revised form 17 March 2008
Accepted 27 March 2008
Available online 8 April 2008

Keywords:
Red mud
Iron recovery
Building material
Mineral transformation
Reuse

ABSTRACT

Red mud is a solid waste produced in the process of alumina extraction from bauxite. In this paper, recovery iron from Bayer red mud was studied with direct reduction roasting process followed by magnetic separation, and then building materials were prepared from alumosilicate residues. After analysis of chemical composition and crystalline phase, the effects of different parameters on recovery efficiency of iron were carried out. The optimum reaction parameters were proposed as the following: ratio of carbon powder: red mud at 18:100, ratio of additives: red mud at 6:100, roasting at 1300 °C for 110 min. With these optimum parameters, total content of iron in concentrated materials was 88.77%, metallization ratio of 97.69% and recovery ratio of 81.40%. Then brick specimens were prepared with alumosilicate residues and hydrated lime. Mean compressive strength of specimens was 24.10 MPa. It was indicated that main mineral phase transformed from nepheline ($NaAlSiO_4$) in alumosilicate residues to gehlenite ($Ca_2Al_2SiO_7$) in brick specimens through X-ray diffraction (XRD) technology. The feasibility of this transformation under the experimental conditions was proved by thermodynamics calculation analysis. Combined the recovery of iron with the reuse of alumosilicate residues, it can realize zero-discharge of red mud from Bayer process.

1. Introduction

With the increasing demand both in China and abroad, many alumina plants have sprung up in China in recent years. The total production of alumina in China added up to 13.7 million tons in 2006 which had increased 60% compared with that of 2005 [1]. China ranked the second place among alumina production countries in the world following Australia. Red mud is a solid waste in the production of alumina by alkaline leaching process of bauxite. Generally, 1–1.5 tons of red mud will be produced with each ton of alumina production. And there are approximately 15 million tons of red mud produced in China every year.

Red mud characterizes to be of high alkalinity, so it can cause serious environment problems. Alkaline solution and red mud slurry usually seep from the red mud landfill site or pipelines into ground or underground water. Huge areas of land are required for the storage of red mud, which may cause the reduction of farming land. And building and maintenance of red mud dam need a lot of money. An alumina plant in Shandong province spent 70 million Yuan on a red mud landfill project in China [2].

Characteristics of red mud differ from different processes of alumina production [3]. Red mud from sintering process, containing some reactive substance such as β-$2CaO{\cdot}SiO_2$, can be used to produce construction materials directly [2,4,5]. However, in Bayer process, Al_2O_3 is dissolved depending on sodium hydroxide from high-iron, high-aluminum boehmite and gibbsite bauxite without calcination. Thus there is less pozzalanic active substance in the Bayer red mud. It is not feasible to use red mud from Bayer process as construction materials directly. Some research work on calcination cement was carried out with Bayer red mud by Tsakiridis et al. [6]. However, only 3–5% red mud can be mixed with other raw materials and it is not an effective way compared with the huge amount of the production of red mud. Pontikes et al.[7] did some research work in producing ceramic with Bayer red mud, which has the potential of utilization red mud in industries. Some techniques of recovery rare elements from red mud are not applied because of those complicated procedure and high cost, although some useful production such as gallium, titanium dioxide, and scandium can be obtained [8–10]. As the high iron content of the Bayer red mud, some researches were carried out on recovery iron from them [11–14]. In this approach, iron can be recovered with simple treatment, i.e. reduction. It should be noted that alumosilicate residues, after the recovery of iron, are up to 60% of total amount of red mud, and they also face the problem of storage and secondary pollution. In this thesis, iron was recovered from red mud of Bayer

* Corresponding author. Tel.: +86 27 87792207; fax: +86 27 87792101.
E-mail address: yjiakuan@hotmail.com (J. Yang).

0304-3894/$ – see front matter © 2008 Elsevier B.V. All rights reserved.
doi:10.1016/j.jhazmat.2008.03.122

Table 1
Chemical composition of red mud

Components	SiO_2	Fe_2O_3	Al_2O_3	CaO	MgO	TiO_2	Na_2O	K_2O	SO_4^{2-}	LOI
Content (wt%)	20.98	27.93	22.00	6.23	1.32	2.3	10.5	0.04	0.6	9.96

process with direct reduction roasting and building materials were prepared with alumosilicate residues magnetically separated from red mud.

2. Experiment

2.1. Experimental theory

Direct reduction process for direct reduction iron (DRI) consists of gas-based reduction process and coal-based reduction process. In the gas-based process, deoxidization reaction is done in shaft furnace, tank furnace or fluidized bed boiler with a reducing gas of H_2 or CO. FASMET is the most common coal-based method in China, in which coal acts as reducing agent and deoxidization reaction is completed in rotary kiln or tunnel kiln [15]. The reaction theory can be expressed with the following equations [16]:

$$Fe_2O_3 + 3C \rightarrow 2Fe + 3CO\uparrow \quad (1)$$

$$Fe_3O_4 + 4C \rightarrow 3Fe + 4CO\uparrow \quad (2)$$

$$FeO + C \rightarrow Fe + CO\uparrow \quad (3)$$

Taking Eq. (3) as an example, the relationship between reduction degree and parameters is shown in Eq. (4) [17],

$$t_R = R'/[AKM_c^{\bullet}\exp(-E/R^0T)] + r_0'\rho_0^{\bullet}[1/2 - R'/3 - (1-R')^{2/3}/2]/3D_e \quad (4)$$

In Eq. (4), t_R is the time of iron oxide reduction (s), R' is reduction degree of production (%), A is reaction constant, E is activation energy (J mol^{-1} K^{-1}), R^0 is the ideal gas constant (8.314 J mol^{-1} K^{-1}), T is the temperature (K), K is the balance constant of iron reduction equation, M_c is coal ratio (%), r_0' is grain radius when reduction degree is R' (m), ρ_0 is oxygen contain in iron oxide initially (mol m^{-3}), and D_e is diffuse coefficient in solid phase (m^2 s^{-1}).

From Eq. (4), the parameters that influence reduction degree of reaction are reaction temperature, reaction duration, and ratio of carbon. Moreover, red mud contains many impurities, such as SiO_2, Al_2O_3, which can have the negative impact on the reduction reaction between FeO and carbon. Mei et al. found that calcium and magnesium carbonate can react with these impurities and improve reduction ratio of FeO [18]. In summary, main factors on iron recovery were ascertained as: reaction temperature, reaction duration, carbon ratio, and additive ratio.

2.2. Raw materials

Red mud from Bayer process was sampled from red mud storkyard of an alumina plant in Chiping of Shandong Province, China. Chemical and mineral compositions and ferrous chemical phase of red mud samples were analyzed. Results of chemical analysis showed that compositions of red mud comprise Fe_2O_3, SiO_2, Al_2O_3, CaO, Na_2O, and TiO_2 (Table 1). The crystalline phases were investigated by powder XRD technique, using Ni-filtered Cu Kα, operated at 40 kV and 30 mA and at the rate of 4° min^{-1}. Some mineral phases exist, such as quartz, hematite, limonite, cancrinite, calcite, and illite, shown in Fig. 1. According to the chemical phase analysis, most of iron existed as hematite (Fe_2O_3) and limonite ($nFe_2O_3{\cdot}mH_2O$), followed by ferrosilite ($FeSiO_3$), siderite ($FeCO_3$) and pyrites (FeS) (Table 2).

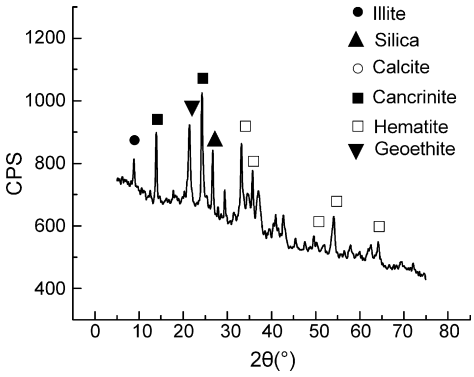

Fig. 1. XRD pattern of Bayer red mud.

In order to eliminate the negative effect of carbon on iron recovery experiment [17], commercial analysis grade activated carbon was used as reducing agent. The additives were made by analysis grade calcium carbonate mixed with equal magnesium carbonate.

Lime was used as an activator in the preparation of brick specimens, and supplied by the alumina plant as a by-product in the production of CO_2. Lime should be slaked before application.

2.3. Experimental method

Four group experiments were designed to investigate the effects of different parameters on iron recovery from red mud, such as roasting temperature, roasting time, the ratio of carbon to red mud, and the content of the additives. Red mud was mixed thoroughly with carbon and additives according to specific proportions and then the mixture was pressed with a cylinder mold I (Φ 20 mm × 40 mm) by press machine at a pressure of 10 MPa. The shaped columnar samples were put in crucibles, then dried and roasted at high temperature in furnace. After a given time, roasted samples were taken out and quenched with water immediately. Products were milled and separated by magnetic separator (model: XCGS-79), with working electrical current of 1 A. The content of total iron (T_{Fe}) and content of metallic iron (M_{Fe}) of magnetically separated concentrate were analyzed in chemistry method. Then metallization ratio (M_{Fe}/T_{Fe}) was calculated, and recovery ratio of iron (the ratio of the amount of iron in magnetically separated concentrate to that in red mud raw material) were deduced according to mass balance in magnetic separation process.

The element compositions of both the concentrate and alumosilicate residues were analyzed by X-ray fluorescence (XRF, EAGLE III, by EDAX). XRF was carried out with Rh target, Si (Li) crystal detector and calibrated by fundamental parameters.

The alumosilicate residues after magnetic separation and the slaked lime were mixed together and then the mixture was pressed

Table 2
Chemical phases of iron in red mud

Phase	Hematite (limonite)	Ferrosilite	Siderite	Pyrites	T_{Fe}
Fe (%)	19.24	0.23	0.05	0.03	19.55
Fe/T_{Fe} (%)	98.41	1.18	0.26	0.15	100.00

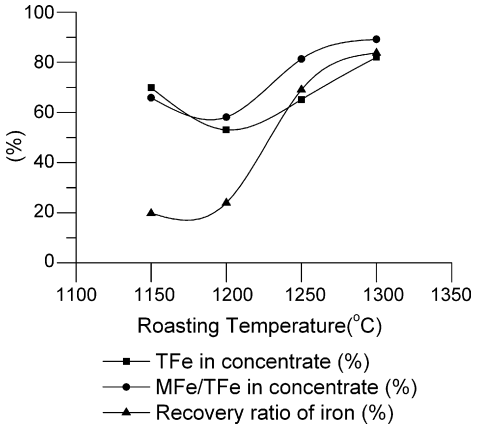

Fig. 2. Effects of the roasting temperatures on iron recovery.

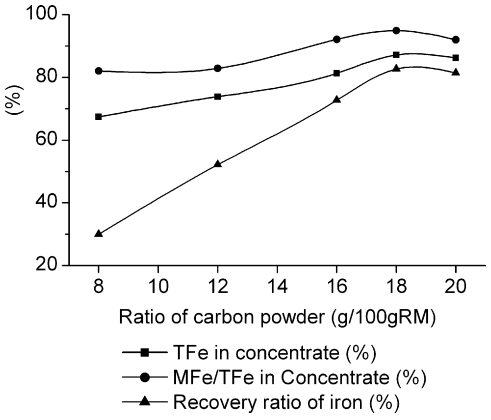

Fig. 4. Effects of the content of carbon powder on iron recovery.

with a shape of cylinder mold II (Φ 30 mm × 50 mm) by a press machine at a pressure of 20 MPa. The samples were controlled with the same weight and high. Then samples were cured with the steam of 80 °C under 1 atm for 11 h in braising-boiler (model: YXQ-LS-50SII). The compressive strengths of cured samples were tested after dipped in water for 24 h. The crystalline phases of alumosilicate residues and cured brick specimens were comparatively investigated by powder XRD technique. The experimental conditions of XRD were the same as presented in Section 2.2.

3. Results and discussion

3.1. Iron recovery

3.1.1. Effect of temperature on iron recovery

Samples consisted of red mud, carbon and additive at a proportion of 100: 18:6, and were roasted 110 min at a series of different temperatures such as 1150, 1200, 1250 and 1300 °C, respectively. The effects of roasting temperatures on T_{Fe}, degree of metallization, and ratio of iron recovery were shown in Fig. 2.

From Fig. 2, T_{Fe} and metallization degree (M_{Fe}/T_{Fe}) at 1200 °C were lower than that at 1150 and 1250 °C obviously. At 1150 °C or higher, low melting point substances such as $2FeO{\cdot}SiO_2$, $2FeO{\cdot}Al_2O_3$ and $2FeO{\cdot}2Al_2O_3{\cdot}5SiO_2$ were generated through the reaction among FeO and SiO_2 or Al_2O_3. Because of these substances, the reactive activity of the reactant was decreased, and reduction of iron oxide and the growth of metallic iron crystalline were blocked. With the active effect of the additives at temperature higher than 1200 °C, these cumbers of lower melting point substances would be broken, and T_{Fe} and M_{Fe}/T_{Fe} improved when roasting temperature was 1300 °C.

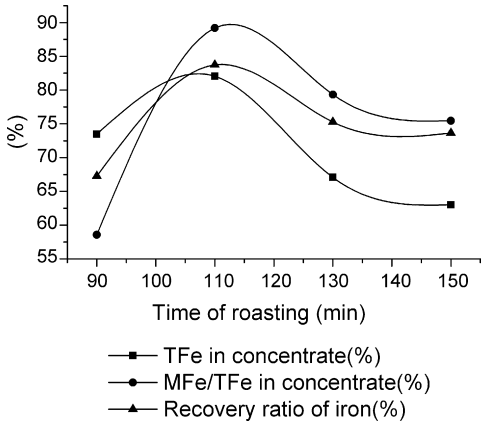

Fig. 3. Effects of roasting time on iron recovery.

3.1.2. Effects of roasting time on iron recovery

Samples were roasted at the temperature of 1300 °C for different roasting time, with the same proportion of red mud, carbon and additive at 100:18:6. Experimental results were shown in Fig. 3.

As shown in Fig. 3, there was non-linear relationship between each parameter of iron recovery and roasting time, with each parameter of iron reduction achieving a peak when roasting time was about 110 min. It was inferred that the optimum roasting time was about 110 min, during which deoxidization reaction of ferrous oxides was mostly completed.

3.1.3. Effects of ratio of carbon to red mud on iron recovery

In order to investigate the optimum content of carbon, different ratios of carbon to red mud were studied, respectively, and other experiment parameters were kept as the following: the ratio of additive: red mud at 6:100, reduction temperature of 1300 °C for 110 min. Results were shown in Fig. 4.

As shown in Fig. 4, three parameters of iron recovery rose with the increase of the ratio of carbon to red mud. When the ratio of carbon to red mud was over 18:100, T_{Fe}, M_{Fe}, and recovery ratio of iron kept stable. In case of calculation as hematite contained in red mud, only 6.3% carbon was needed theoretically, which was much less than experimental data. It was indicated that some carbon reacted with the impurities of red mud simultaneously.

3.1.4. Effects of the content of additives on iron recovery

Low melting-point iron phase would be generated by impurities in red mud at high temperature. If additives of $CaCO_3$ or $MgCO_3$ were added, $CaO{\cdot}SiO_2$, $MgO{\cdot}SiO_2$ would be firstly formed between impurities and CaO or MgO, the decomposed production of $CaCO_3$ or $MgCO_3$. As a result, reactive of reduction of iron oxides was improved. Effects of the content of the additives on three parameters (T_{Fe}, M_{Fe}, and recovery ratio of iron) were shown in Fig. 5. As shown in Fig. 5, generally the optimum content of the additive was about 6%. In this series of experiments, other parameters were kept as following: the ratio of carbon powder: red mud at 18:100, roasting at 1300 °C for 110 min.

3.1.5. Composition analysis of the concentrate and alumosilicate

Above all, optimum conditions were suggested as following: roasting temperature of 1300 °C, roasting time of 110 min, the carbon to red mud mass ratio of 18:100, the additives to red mud mass ratio of 6:100. Under the optimum conditions, red mud samples

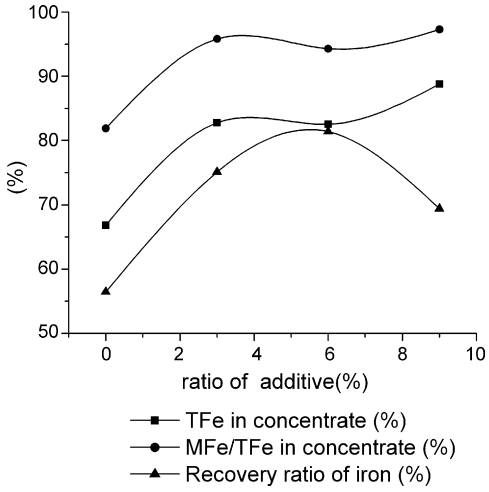

Fig. 5. Effects of content of the additives on iron recovery.

Table 3
Element compositions of the concentrate and the residues from magnetic separation (wt%)

Element	Fe	Si	Al	Ca	Mn	Na	Mg	Ti
Concentrate	89.05	3.75	6.43	0.54	0.23	–	–	–
Residues	5.78	37.26	34.08	6.42	–	11.59	1.55	3.32

were roasted, reduced, milled and magnetically separated in turn. Then the chemical compositions of the concentrate and alumosilicate residues were analyzed through XRF. The results were shown in Table 3. T_{Fe} and M_{Fe} in concentrate were analyzed by chemistry method. Three parameters of iron recovery were summarized as: T_{Fe} 88.77%, metallization rate 96.98%, and iron recovery rate of 81.40%. It was indicated that the recovery products of magnetic separation process could be used as direct reduction iron in the metallurgical production of steel products.

3.2. Preparations of bricks with alumosilicate residues

3.2.1. Chemical compositions and mineral phases of alumosilicate residues

In optimum conditions mentioned above, alumosilicate residues from magnetic separation process were collected for reuse of building materials. Chemical compositions of the residues were shown in Table 3, and the XRD pattern of the residues was shown in Fig. 6(A). As shown in Table 3, oxides of Si, Al, and Ca were useful compositions that could be used to the preparation of

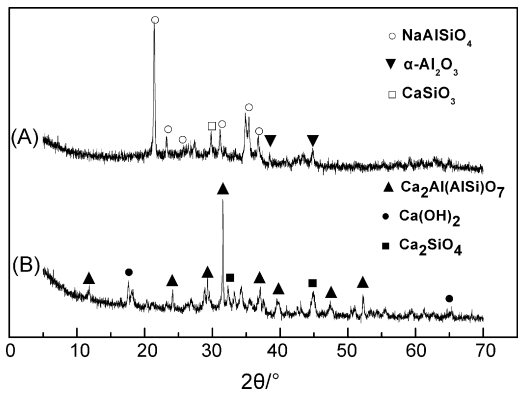

Fig. 6. XRD patterns of alumosilicate residues (A) and tested cured specimens (B).

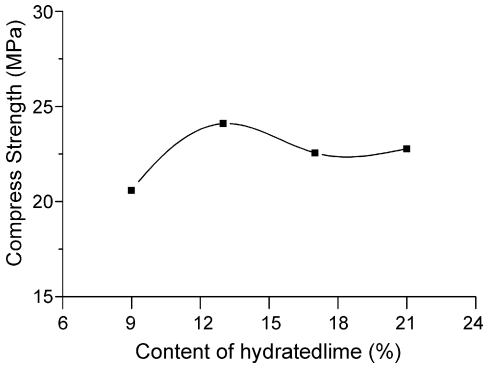

Fig. 7. Effects of the content of hydrated lime on compressive strength.

brick. As shown in Fig. 6, the main crystalline phases of residues were $NaAlSiO_4$, α-Al_2O_3 and $CaSiO_3$.

3.2.2. Effect of the content of lime on compressive strength of brick specimens

Lime is a common and cheap alkaline activator of hydrated reaction. The different content of hydrated lime of 9%, 13%, 17% and 21% were added into and mixed with the alumosilicate residues. After molding and autoclaving process, compressive strength of samples was tested, shown in Fig. 7. Some other properties of brick specimens of Chinese standard dimension in size of 240 mm × 115 mm × 53 mm, such as durability and flexural strength, will be studied systematically in further research.

As shown in Fig. 7, compressive strength of samples reached a maximum peak of 24.10 MPa at the content of hydrated lime of about 13%. The XRD patterns of both the original residues and cured brick specimens were comparatively shown in Fig. 6. It was clear that main crystalline phase transferred from nepheline ($NaAlSiO_4$) in the original residues to gehlenite ($Ca_2Al_2SiO_7$) and calcium silicate (Ca_2SiO_4) in the cured samples. Both gehlenite and calcium silicate have definitely stability and strength, so it showed the feasibility of preparation of bricks from the residues.

3.2.3. Preliminary investigation on phase transformation mechanism of cured bricks

In cured stage, the phase transformation process could be expressed as Eq. (5).

$$2NaAlSiO_4 + 2Ca(OH)_2 \rightarrow Ca_2Al_2SiO_7 + Na_2SiO_3 + 2H_2O \quad (5)$$

The transformation relationship between nepheline and gehlenite as shown in Eq. (5) has not been reported in previous literatures. The feasibility of the reaction was proved through calculating Gibbs free energy. Based on classical thermodynamics formula, Eq. (6),

$$\Delta G = \sum v_j G_j(\text{productions}) - \sum v_i G_i(\text{reactants}) \quad (6)$$

if $\Delta G < 0$, the reaction is possible in the relevant conditions.

Table 4
Gibbs free energy of the relative phases (T = 80 °C)

Substance	ΔG_f (kJ mol^{-1})
$NaAlSiO_4$[a]	−2054.42
$Ca(OH)_2$	−1016.42
$Ca_2Al_2SiO_7$[b]	−4053.91
$Na_2O{\cdot}SiO_2$	−1602.60
H_2O (l)	−280.68

[a] Calculated as published by Shi et al. [19].
[b] Calculated as Li et al. [20], else refer Liang et al. [21].

Some values of Gibbs free energy of reactants and products involved were listed in Table 4. Substituted the data in Table 4 to Eq. (6), $\Delta G|_{T=80\,^{\circ}C}$ could be deduced as $-76.19\,kJ\,mol^{-1}$. It was indicated that the phase transformation reaction was possible in the temperature of 80 °C. It was consistent with the results of XRD patterns.

Furthermore, in the Eq. (5), sodium silicate is a common alkaline bond. Through the transformation from soluble Na_2CO_3 to insoluble $NaAlSiO_4$ and $NaSiO_3$, sodium was stabilized and could be difficult in leaching from bricks.

4. Conclusion

(1) Major chemical compositions of red mud were Fe_2O_3, SiO_2, and Al_2O_3. Quartz, hematite, limonite, cancrinite, calcite, and illite existed in red mud as main mineral phases, and most of iron existed in hematite-limonite ore, accompanied with some $FeSiO_3$, $FeCO_3$, and FeS.

(2) Roasting temperature, reduction time, the ratio of carbon to red mud, and content of the additive were four main factors which had effects on recovery of iron. Through corresponding four groups of experiments, optimum reduction reaction conditions were obtained as the follows: roasting temperature of 1300 °C, roasting time of 110 min, the ratio of carbon: additives: red mud of 18:6:100. Under the optimum reaction conditions, four parameters of the recovery process of magnetically separated concentration were obtained as the follows: T_{Fe} of 88.77%, metallization ratio of 96.98%, and iron recovery rate of 81.40%.

(3) The brick specimens were prepared from alumosilicate residues after magnetic separation process. The compressive strength of cured brick samples achieved the maximum peak of about 24.10 MPa at the content of hydrated lime of 13%. Main crystalline phases transformed from nepheline in the original residues into gehlenite and calcium silicate in cured brick samples. Thermodynamics calculated results showed that the feasibility of this phase transformation.

(4) Recovery of iron from Bayer red mud was carried out by direct reduction roasting–magnetic separation process. Moreover, the residues after magnetic separation process were reused as building materials. This combination recycling process showed the potential benefits of zero-emission of red mud wastes from the production industry of alumina.

Acknowledgments

The authors thank Analytical and Testing Center of Huazhong University of Science and Technology, which supplied us the facilities to fulfill the measurement. The authors also would like to thank to Dr. John Cram from China-UK HUST-RRes Genetic Engineering and Genomics Joint Laboratory for his guidance in English writing.

References

[1] National Bureau of Statistics of China, National economic and social development statistical bulletin PR. China in 2006. Available at: http://www.stats.gov.cn/tjgb/ndtjgb/qgndtjgb/t20070228_402387821.htm, 2007.
[2] J.K. Yang, C. Fan, J. Hou, B. Xiao, W. Liu, Engineering application of basic level materials of red mud high level pavement, Chin. Mun. Eng. 123 (2006) 7–9 (in Chinese).
[3] Y. Liu, C.X. Lin, Y.G. Wu, Characterization of red mud derived from a combined Bayer Process and bauxite calcination method, J. Hazard. Mater. 146 (2007) 255–261.
[4] G. Xing, J.K. Yang, J. Hou, B. Xiao, Study on compositions of raw materials of the non-fired brick made from red mud and fly ash, Light. Met. 3 (2006) 24–27 (in Chinese).
[5] P.X. Zhang, J.Q. Yan, Making glass-ceramics using red mud as raw materials, Nonferrous Met. 52 (2000) 77–79 (in Chinese).
[6] P.E. Tsakiridis, S. Agatzini-Leonardou, P. Oustadakis, Red mud addition in the raw meal for the production of Portland cement clinker, J. Hazard. Mater. 116 (2004) 103–110.
[7] Y. Pontikes, P. Nikolopoulos, G.N. Angelopoulos, Thermal behaviour of clay mixtures with bauxite residue for the production of heavy-clay ceramics, J. Eur. Ceram. Soc. 27 (2007) 1645–1649.
[8] D.I. Smirnov, T.V. Molchanova, The investigation of sulfuric acid sorption recovery of scandium and uranium from the red mud of alumina production, Hydrometallurgy 45 (1997) 249–259.
[9] M.T. Ochsenkuhn-Petropoulou, K.S. Hatzilyberis, L.N. Mendrinous, C.E. Salmas, Pilot-plant investigation of the leaching process for the recovery of scandium from red mud, Ind. Eng. Chem. Res. 41 (2002) 5794–5801.
[10] J.J. Zhang, Z.G. Deng, T.H. Xu, Experimental study on acid leach of red mud, Light Met. 2 (2005) 13–15 (in Chinese).
[11] L.Y. Li, A study of iron mineral transformation to reduce red mud tailings, Waste Manage. 21 (2001) 525–534.
[12] L. Piga, F. Pochetti, L. Stoppa, Application of thermal analysis techniques to a sample of Red Mud – a by-product of the Bayer process – for magnetic separation, Thermochim. Acta. 254 (1995) 337–345.
[13] X.G. Mei, M.L. Yuan, W.L. Zuo, J. Chen, Kinetics of the nucleation and grain growth of metallic phase in direct reduction of high-iron Red Mud with coal base, J. Cent. South. Univ. Technol. (Nat. Sci.). 27 (1996) 159–163 (in Chinese).
[14] Z.G. Liu, C.S. Yang, Z.H. Cheng, M.J. Ai, Treatment and utilization of red mud derived from Bayer process, Chin. J. Nonferrous Met. 7 (1997) 40–44 (in Chinese).
[15] Y.J. Li, Z.Y. Zhang, Z.T. Yuan, Y.X. Han, Prospect and application state of high grade iron concentrate, Metal. Mine. 11 (2006) 5–7, 16 (in Chinese).
[16] X.H. Huang, Principle of Steel Metallurgy, Metallurgical Industry Press, Beijing, China, 1986.
[17] Y.K. Liu, X.G. Mei, Study on coal-based direct reduction of High-iron-content Red Mud, Sintering Pelletizing 20 (1995) 5–9 (in Chinese).
[18] X.G. Mei, M.L. Yuan, J. Chen, Research on process of coal-based direct reduction of High-iron-content Red Mud, Nonferrous Met. (Extr. Metal.) 2 (1996) 27–30 (in Chinese).
[19] J.G. Shi, G.Z. Lu, G. Cao, A new method of calculating Gibbs free energy of formation of zeolites, J. Chem. Ind. Eng. (China) 57 (2006) 2806–2811 (in Chinese).
[20] X.B. Li, Y.F. Li, X.M. Liu, G.H. Liu, Z.H. Peng, Y.C. Zhai, A simple method of Gibbs free energy and enthalpy of complicate silicates, J. Chin. Ceram. Soc. 29 (2001) 232–237 (in Chinese).
[21] Y.J. Liang, Y.C. Che, X.X. Liu, Inorganic Thermodynamic Data Manual, NEU Press, Shenyang, China, 1993.